

DIFFUSE OPTICAL MEASUREMENT OF HEMOGLOBIN AND CEREBRAL BLOOD FLOW IN RAT BRAIN DURING HYPERCAPNIA, HYPOXIA AND CARDIAC ARREST

Joseph P. Culver^{*}, Turgut Durduran^{*}, Cecil Cheung^{*}, Daisuke Furuya[#], Joel H. Greenberg[#] and A. G. Yodh^{*}

1. Introduction

Tissue viability and function are often manifest in hemodynamic signatures, because metabolism and vascular regulatory mechanisms modulate the concentration, oxygenation and flow characteristics of blood cells. Assessment of tissue viability and function from hemodynamic measures can be complicated however, by the interplay between vascular supply, tissue oxygen consumption and regulatory effects. It is therefore desirable to independently monitor hemoglobin concentration, oxygenation and flow. In this contribution we present diffuse optical measurements of hemoglobin concentration, oxygenation and flow during global modulations in rat brain, through the intact skull.

Several different multi-parameter measurement schemes have already been employed in rat brain models of functional activation. For example functional magnetic resonance imaging (fMRI) measures of blood oxygen (BOLD), cerebral blood volume (CBV), and cerebral blood flow (CBF) have been combined to calculate oxygen metabolism $CMRO_2$ [6] during rat forepaw stimulation. In a different vein, near surface optical techniques have been used in exposed cortex preparations, for example combining optical spectroscopy and laser Doppler flowmetry [7], or combining phosphorescence oxygen sensors with laser Doppler flowmetry [1]. In our work we employ deep tissue near infrared (NIR) technologies [8] and a novel correlation spectroscopy measure of blood flow. The near infrared methodologies are minimally invasive and performed with the skull intact. We present data derived from models of

^{*} Department of Physics and Astronomy, [#] Cerebrovascular Research Center, Department of Neurology, University of Pennsylvania, Philadelphia, PA 19104

hypercapnia, hypoxia and cardiac arrest; changes in rCBF, hemoglobin concentration and oxygenation are discussed.

2. Methods

We briefly review our methodology. A more detailed description is found in [3].

2.1. Instrument

Near infrared spectroscopy with diffuse photon density waves (DPDW) was used to measure tissue oxy- and deoxy-hemoglobin concentrations, and diffuse light correlation spectroscopy was used to measure tissue blood perfusion. The diffuse photon density wave measurements employed two intensity modulated (70Mhz) laser diodes (786nm and 830nm). Light reflected from the tissue was detected by four avalanche photodiodes and demodulated to deduce amplitude and phase variations. The diffuse light correlation flowmetry measurements utilized a single mode, large coherence length (>1m) laser source operating at 790nm. Single mode fibers were used to relay image single speckles to avalanche photodiodes, and a correlator chip analyzed the time variant speckle intensity to obtain the temporal intensity autocorrelation functions. All three lasers were multiplexed onto a two-dimensional 3x3 grid (8mmx10mm) of nine optical fibers located in the image plane of a camera. A relay lens projected the probe grid onto the sample (e. g. rat cranium) permitting non-contact measurements. DPDW measurements were interlaced between successive diffuse correlation measurements.

2.2. Theory

We take the measurement plane to coincide with the xy-plane, which is normal to the z-axis. The transport of diffuse photon density waves ($\Phi(\rho)$) is modeled using an extrapolated zero boundary condition, semi-infinite media approximation with solutions [5] of the form

$$\Phi(\mathbf{r}) = \frac{3\mathbf{m}_s' S_o}{4\mathbf{p}} \left(\frac{e^{ikr_1}}{r_1} - \frac{e^{ikr_2}}{r_2} \right)$$

Here $k^2 = 3\mathbf{m}_s'(i\omega/\mathbf{v} - \mathbf{m}_a)$, k is complex wavenumber of the DPDW, μ_a is the tissue absorption coefficient, μ_s' is the tissue scattering coefficient, ω is the modulation frequency, and \mathbf{v} is the speed of light in the medium.

$r_1 = \sqrt{\mathbf{r}^2 + z_o^2}$, $r_2 = \sqrt{\mathbf{r}^2 + (z_o + 2z_B)^2}$, ρ is the source detector separation along the surface, z_o is $\sim 1/\mu_s'$, and z_B , the extrapolated zero boundary distance, corresponds to the distance above the tissue surface at which the light fluence extrapolates to zero. The data was fit to the expression above to extract wavelength-dependent tissue absorption, and then spectral decomposition was used to extract the hemoglobin concentrations ([Hbr], [HbO₂]) from the tissue absorption assuming a 50/50 water/lipid background absorption ratio.

The diffuse light electric field autocorrelation function ($G(\rho, \tau)$) was analyzed in a similar way. The primary difference is that the wavenumber, k_D , associated with $G(\rho, \tau)$, depends on the autocorrelation time, i.e., $k_D^2 = 3m_s' m_a + 6m_s'^2 m_a^2 k_o^2 \alpha D_B \tau$; here τ is the autocorrelation time delay, k_o is the optical photon's wavenumber in the medium. The probability that a photon is scattered by a moving "cell", α , is presumed proportional to cerebral blood volume [3]. The blood flow speed is parameterized by a Brownian diffusion constant D_B and the product αD_B parameterizes blood flow. The correlation measurement gives αD_B .

2.3. Experiments

Adult male Sprague-Dawley rats weighing 300-325 g were fasted overnight prior to measurements. The animals were anesthetized (Halothane 1-1.5%, N₂O 70%, O₂ 30%) and catheters were placed into a femoral artery to monitor the arterial blood pressure and into a femoral vein for drug delivery. The body temperature was maintained at 37±2C. The animal was tracheotomized, mechanically ventilated and fixed on a stereotaxic frame. The scalp was reflected since the fur introduced a slight distortion onto the near-infrared signals. The probe was placed symmetrically about midline and covered a region from 2mm anterior to 6mm posterior of the rhinal fissure. Following the surgical procedures, halothane was withdrawn and anesthesia was maintained with α -chloralose (60 mg/kg), followed by supplemental doses of 30 mg/kg every hour. The hypercapnic challenge consisted of elevating blood p_aCO₂ by adding carbon dioxide (8%) into the breathing mixture. The hypoxic modulation involved decreasing the arterial p_aO₂ by reducing the inspired O₂ to 10%. Cardiac arrest was achieved with a 1 mL, 3 M solution of KCL.

3. Results

Figure 1 shows the percent increase from the baseline level of αD_B in one experiment where the animal breathed 8% CO₂ for 10 minutes. The numbers shown in the figure were averaged over the area of the imaged brain, which comprised an 8x10 mm² area of cortex. During the CO₂ inhalation, the p_aCO₂ increased from 38 mmHg to 75 mmHg, and the average relative increase of αD_B was about 0.77 (77%) from the baseline. Figure 1 also shows the concurrent changes in the hemoglobin concentration averaged over the same cortical area. A 0.17 (17%) increase in the hemoglobin concentration was observed. The hemoglobin concentration apparently increases at a slower rate than αD_B and also decays more slowly after the CO₂ was switched off. The average relative increase of hemoglobin oxygenation in the cortex during the same CO₂ stimulation is shown in the bottom panel of Figure 1. The increase was about 16%; the oxygenation dynamics followed the flow changes more closely than the total hemoglobin concentration. We also obtained time courses for hypoxia and cardiac arrest (not shown). In Figure 1, the relative changes averaged over

the last 10 minutes of the hypercapnia are plotted along with the relative changes during hypoxia and cardiac arrest. The values are obtained by averaging the signal from 5 to 15 minutes following the perturbation.

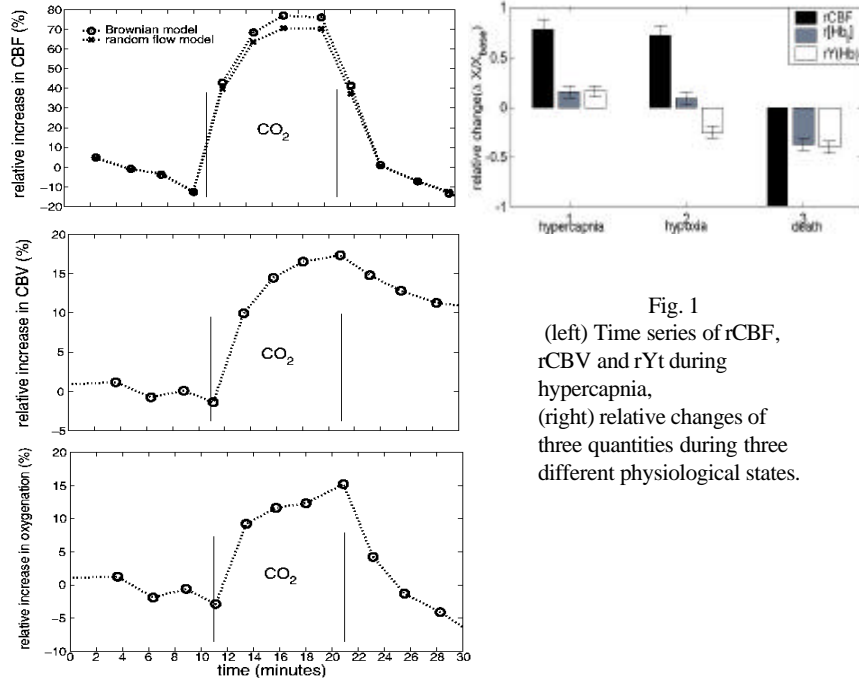


Fig. 1
 (left) Time series of rCBF, rCBV and rYt during hypercapnia,
 (right) relative changes of three quantities during three different physiological states.

4. Discussion

Vasodilatation increased blood flow (CBF) and blood volume (CBV) in both hypercapnia and hypoxia. Since oxygen metabolism remains roughly constant during hypercapnia and hypoxia, the flow increases are countered by a reduced oxygen extraction fraction. The measured tissue saturation (Y_t) is a combination of arterial, capillary, and venous tissue compartments. During hypercapnia the arterial saturation is constant so that the reduced oxygen extraction fraction results in increased tissue saturation, while during hypoxia, the drop in arterial saturation results combined with a decreased oxygen extraction fraction results in decreased tissue saturation. Cardiac arrest completely stops blood flow although the oxygen saturation does not go to zero. From these three modulations we have measured three different trends in the hemoglobin saturation and blood flow.

5. Summary

We have demonstrated the ability to concurrently measure relative changes in cerebral blood flow, hemoglobin concentration, and hemoglobin oxygenation

with a single non-contact, non-invasive instrument. Our measurements from rat hypercapnia, hypoxia and cardiac arrest models are in reasonable agreement with the literature, and offer the possibility for further growth and quantification. The optical techniques used in this study are attractive also because they enable experimenters to measure vascular response of deep tissues. The new instrument and concept may also be applicable to human studies especially in infants and neonates permitting noninvasive monitoring of cerebral hemodynamics and oxygen (see [4] and [2] for examples of NIR spectroscopy).

We gratefully acknowledge support from grants NIH RO1-HL57835-01.

6. References:

- [1] Ances, B.M., Wilson, D.F., Greenberg, J.H. and Detre, J.A., Dynamic changes in cerebral blood flow, O₂ tension, and calculated cerebral metabolic rate of O₂ during functional activation using oxygen phosphorescence quenching, *Journal of Cerebral Blood Flow and Metabolism*, 21 (2001) 511-516.
- [2] Benaron, D.A., Hintz, S.R., Villringer, A., Boas, D., Kleinschmidt, A., Frahm, J., Hirth, C., Obrig, H., van Houten, J.C., Kermit, E.L., Cheong, W.F. and Stevenson, D.K., Noninvasive functional imaging of human brain using light, *Journal of Cerebral Blood Flow and Metabolism*, 20 (2000) 469-477.
- [3] Cheung, C., Culver, J.P., Yodh, A.G., Takahashi, K. and Greenberg, J.H., In vivo cerebrovascular measurement combining diffuse near-infrared absorption and correlation spectroscopies, *Physics in Medicine and Biology*, 46 (2001) 2053-2065.
- [4] Danen, R.M., Wang, Y., Li, X.D., Thayer, W.S. and Yodh, A.G., Regional imager for low-resolution functional imaging of the brain with diffusing near-infrared light, *Photochemistry and Photobiology*, 67 (1998) 33-40.
- [5] Haskell, R.C., Svaasand, L.O., Tsay, T.T., Feng, T.C. and McAdams, M.S., Boundary-Conditions For the Diffusion Equation in Radiative- Transfer, *Journal of the Optical Society of America a-Optics Image Science and Vision*, 11 (1994) 2727-2741.
- [6] Mandeville, J.B., Marota, J.J.A., Ayata, C., Moskowitz, M.A., Weisskoff, R.M. and Rosen, B.R., MRI measurement of the temporal evolution of relative CMRO₂ during rat forepaw stimulation, *Magnetic Resonance in Medicine*, 42 (1999) 944-951.
- [7] Mayhew, J., Johnston, D., Berwick, J., Jones, M., Coffey, P. and Zheng, Y., Spectroscopic analysis of neural activity in brain: Increased oxygen consumption following activation of barrel cortex, *Neuroimage*, 12 (2000) 664-675.
- [8] Villringer, A. and Chance, B., Non-invasive optical spectroscopy and imaging of human brain function, *Trends in Neurosciences*, 20 (1997) 435-442.